

Research Article

Synthesis of Electrospun Polyvinyl Butyral/Bentonite Nanofiber Film for Cationic Dye Removal

Aiizat Ikhwan Abdul Jalil ¹, Syahida Farhan Azha ¹, Adrian Bonilla-Petriciolet ²,
Mohammad Shahadat ³ and Suzylawati Ismail ¹

¹School of Chemical Engineering, Engineering Campus, Universiti Sains Malaysia, Nibong Tebal 14300, Penang, Malaysia

²Instituto Tecnológico de Aguascalientes, Aguascalientes 20256, Mexico

³School of Chemical Sciences, Universiti Sains Malaysia, Nibong Tebal, Penang 11800, Malaysia

Correspondence should be addressed to Mohammad Shahadat; mdshahadat93@gmail.com and Suzylawati Ismail; chsuzy@usm.my

Received 8 December 2022; Revised 3 February 2023; Accepted 7 February 2023; Published 15 March 2023

Academic Editor: Senthil Kumar Ponnusamy

Copyright © 2023 Aiizat Ikhwan Abdul Jalil et al. This is an open access article distributed under the Creative Commons Attribution License, which permits unrestricted use, distribution, and reproduction in any medium, provided the original work is properly cited.

The textile industry is a common and relevant sector worldwide that generates significant environmental pollution via the discharge of dye-containing wastewater. In this direction, the electrospinning technology can be used to produce adsorbing nanofibers for the treatment of wastewater polluted by dyes and other toxic compounds. The nanofibers obtained by this technology are light and thin, thus providing several advantages (e.g., high surface area) to improve the efficacy of adsorption processes. In this direction, this study reports the preparation of nanofibers from polyvinyl butyral (PVB) and bentonite via electrospinning. This study also reports PVB/bentonite nanofiber mat and its application in adsorbing the cationic dye (methylene blue) from an aqueous solution. The morphology and water contact angles of these nanofibers were analyzed. Results showed that the maximum dye adsorption of these nanofibers was 66.63 mg/g along with 32% removal at pH 9 and $27 \pm 2^\circ\text{C}$. The dye adsorption on these nanofibers was exothermic and pH-dependent, with the best adsorption capacities obtained under alkaline conditions. The adsorption mechanism of this dye molecule on these PVB/bentonite nanofiber mats was associated with van der Waals forces, hydrogen bonding, and electrostatic interactions. This novel composite is an interesting material with improved properties that can be applied to the removal of cationic dyes from wastewater.

1. Introduction

The problem of water pollution cannot be separated from the growth of industrial production. One of the most prominent producers of coloured wastewater is the textile industrial sector. These types of industries implement numerous chemicals in their processes, and their wastewater also contains toxic compounds and anionic and cationic dyes. These dyes can be carcinogenic, mutagenic, and toxic to humans, animals, and plant life, thus significantly affecting ecosystems and the environment. Several conventional methods such as precipitation, coagulation, and oxidation have been implemented to treat the wastewater from the textile sector. Adsorption is one of the most effective

alternatives using inexpensive materials to purify fluids polluted by dyes and other compounds.

Bentonite is a natural clay that has been used extensively as an adsorbent for the industrial treatment of dye-polluted fluids. Bentonite is a montmorillonite composed of 2:1 dioctahedral smectite with an octahedral alumina layer between two tetrahedral silica sheets. It is a mineral that has a high cation exchange capacity, a high specific surface area, and is also physically and chemically stable [1]. Several researchers have implemented bentonite in wastewater treatment. For example, Sahin et al. [2] used cold plasma treatment to modify the surface chemistry of this clay and improve the removal of methylene blue (MB) from the aqueous solution. Results showed that this modified clay

achieved high dye adsorption. Azha et al. [3] prepared an adsorbent coating using acrylic polymer and bentonite for MB removal. The adsorption thermodynamics of MB onto bentonite was analyzed by Hong et al. [4], and they found that this process was spontaneous and endothermic. Bentonite was also used to improve the removal of phenol and chromium ions with persulfate, where high removal efficiencies were obtained [5]. Bentonite was employed to prepare a composite of poly(acrylic acid-acrylic sodium) via copolymerization reactions by You et al. [6]. This composite was used for the removal of cadmium ions with 99.9% removal efficiency.

Electrospinning has been used to prepare novel materials for different applications, including environmental protection and remediation. Electrospun nanofibers have increased use in many fields such as universal membranes, biomedical devices (scaffolding and wound dressing), composite reinforcement, and high surface area fabrics for protective clothing and sensors [7, 8]. Nanofibers formed from the electrospinning process have a large surface area because of their small diameter, and they are porous in nature because of their exceptional pore interconnection. The polymer and electrospinning equipment are relevant and are parameters that affect fiber formation. The polymer properties (e.g., viscosity, concentration, surface tension, conductivity, and molecular weight) have a significant impact on the fiber preparation. In the case of electrospinning equipment, the tip-to-collector distance, voltage intensity, flow rate, collecting roller speed, temperature, and humidity play a fundamental role in the smooth electrospinning procedure. Overall, the process of electrospinning employs an electrical charge to draw the polymer from the syringe to the collector by forming an electric field. From the electric force provided, a Taylor's cone would form on the tip of the needle, and a charged fluid jet would be shot from the apex of the cone. As the jet travels in the air, its diameter decreases due to the evaporation of the solvent, stretching of the jet, and the extension rate [9].

In this direction, polyvinyl butyral (PVB) is odourless, nontoxic, and environmentally friendly, and consequently it can be used as a binder in the electrospinning process. The chemical structure of PVB is given in Figure 1. It also has flexibility, optical clarity, and adhesive strength. Its good compatibility with both polar and nonpolar components is due to the butyral, hydroxyl, and acetyl functional groups. The two groups in PVB (i.e., butyral and vinyl butyral) are hydrophilic and hydrophobic. Consequently, this resin has good compatibility with inorganic materials [10], and it can help prepare composites using clays (e.g., bentonite), which are versatile adsorbents for water treatment.

Different studies have reported the utilization of PVB in electrospinning. For instance, Yener and Yalcinkaya [11] studied the electrospinning of PVB, focusing on the effects of different solvents and concentrations. They found that high concentrations resulted in high polymer chain entanglement, whereas low concentrations resulted in low fiber diameter and beads forming once used with acetic acid, dimethylformamide, and butanol as solvents. Stenicka et al. [9] studied the dissolution of PVB with methanol and

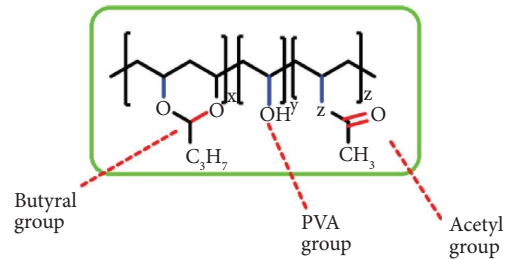


FIGURE 1: Chemical structure of polyvinyl butyral.

isopropanol, thus showing that methanol was a poor solvent, and isopropanol was the best solvent. They also found that the poor solvent had better spinnability and lesser bead formation, thus resulting in a better quality for the electrospun fiber. A similar finding was reported by Peer et al. [7], where the electrorheological performance of PVB solutions was analyzed. These authors used several concentrations of PVB (6, 8, 10, and 12 wt%) and solvents (methanol, ethanol, isopropanol, and butanol), and their results agreed with the classification of poor and good solvents made by Stenicka et al. [9]. The quality of the nanofibers significantly deteriorated with good solvents, and a high quality could be achieved by using poor solvents [12].

Based on these facts, the objective of this research was to prepare a new composite from bentonite and PVB via electrospinning. The electrospun PVB/bentonite nanofibers were then applied for the removal of MB dye from the aqueous solution. With the implementation of a cheaper and underutilized polymer such as PVB as a nanofiber membrane, a new and alternative path for preparing an economical nanofiber adsorbent for the treatment and purification of wastewater has opened up.

2. Experimental Procedure

2.1. Materials. PVB ($M_w = 60\ 000$ g/mol) was chosen as the binder, and it was obtained from Sigma-Aldrich and BT Science Sdn. Bhd. Synthetic cationic MB dye and bentonite were purchased from Modern Lab Sdn. Bhd., Malaysia. The pH of the solution was adjusted using NaOH (0.1 M) and HCl (0.1 M) solutions and monitored with a pH meter (Elico, Malaysia). Normal distilled water was employed for the dilution and solution preparation.

2.2. Preparation of PVB/Bentonite Electrospinning Nanofibers. A 12 wt% PVB solution was prepared by dissolving the PVB powder in ethanol and stirring at 27°C. After homogeneity was reached, 8 wt% bentonite was added to the polymer solution and stirred to get homogeneity. The ratio to obtain the PVB/Ben solution was found to be 0.4 : 5, where 0.4 g of bentonite is added to 5 g of PVB solution. The PVB/bentonite solution was introduced into a 5 mL syringe with an 18G-sized needle, and this syringe was set up with the syringe pump. The voltage was supplied at 12 kV, and the flow rate was constant at 1.4 mL/h. The distance between the tip to the collector was 10 cm and the rotating drum was 100 rpm. By applying the predetermined voltage, flow rate,

tip-to-collector distance, roller speed, and target volume, Taylors' cone was obtained, and a polymer jet was successfully formed. Note that the jet was influenced by the electromagnetic field and began to spiral towards the collector, where a stable polymer would stay together and form fibers on the collector. The completed nanofibers were then peeled from the aluminium foil, washed, and stored for their characterization and dye adsorption studies. The graphical representation of the electrospinning equipment is shown in Figure 2.

Some physicochemical properties of these nanofibers were determined. The water contact angle of PVB/bentonite nanofibers was recorded using a Ramé-Hart standard goniometer. The analysis of these nanofibers was also performed using scanning electron microscopy with energy dispersive X-ray spectroscopy (SEM/EDX) and an extreme high-resolution field emission scanning electron microscope (XHR-FESEM) Model FEI Verios 460L. Fourier transform infrared (FTIR) spectroscopy analysis was done using FTIR-NICOLET iS10 equipment in the region of 4000 to 400 cm^{-1} .

2.3. Batch Adsorption of MB Dye Using PVB/Bentonite Nanofibers. Batch MB adsorption studies on PVB/Bentonite nanofibers were performed at different operating conditions: initial adsorbate concentrations (100, 125, 150, 175, and 200 mg/L), stirring velocities (500, 1000, and, 1500 rpm), and pH (3, 5, 7, 9, and 11). These adsorption studies were performed with 3 g of nanofibers and 200 mL of dye solution at 27°C. Equilibrium and kinetic studies were also performed at predefined operating conditions to calculate thermodynamic parameters and rates of dye adsorption. A UV-VIS spectrophotometer (HACH DR6000) was used to quantify the MB concentration in all solutions. A material balance was applied to estimate the adsorption capacity (q , mg/g) obtained in all experiments.

3. Results and Discussion

3.1. SEM/EDX Analyses of PVB/Bentonite. The SEM images of PVB/Bentonite nanofibers are shown in Figure 3. This analysis showed that the electrospun PVB/bentonite nanofiber was successfully obtained with thin fibers (600 nm) together with bead formation. It was also corroborated that ethanol was a good solvent for PVB due to the low number of beads formed, as stated in the study of Yener and Yalcinkaya [11]. It was also observed that bentonite was entangled and distributed unevenly between the nanofibers, as shown in Figure 3. The orientation of the nanofibers was found to be random, and from the studies of Mullins et al. [13] and Yin and Xiong [14], random distribution of nanofibers exhibits good flexibility, small pore size, and improves the fiber wetting process.

Results of EDX analysis of PVB/Bentonite nanofibers are shown in Table 1. The presence of carbon (C), oxygen (O), silica (S), and alumina (Al) was identified in the sample. The contents of silica and alumina indicated that bentonite was present in the nanofibers because Al_2O_3 and SiO_2 were the main constituents of this clay. Note that these elements play

an important role in the definition of the adsorption properties of bentonite [15, 16]. The FTIR of the electrospun adsorbent is shown in Figure 4. The stretch that indicates alcohol was found at 3439 cm^{-1} . The vibration bands from 3000 to 2800 cm^{-1} corresponded to the C-H bonds. Note that there was a band found at 2359 cm^{-1} that indicated the presence of carbon dioxide before adsorption, which disappeared after adsorption. The presence of C=C at 1633 cm^{-1} indicated the presence of an arene group. In addition, the FTIR spectrum of PVB/Bentonite nanofibers also showed stretch vibrations at 1450 and 1200 cm^{-1} corresponding to the Al-O-M group. The absorption band at 1050 cm^{-1} was associated with the Si-O-Si group. The stretch vibration band from 900 to 800 cm^{-1} was identified that corresponded to the Si-O and Si-OH groups. The absorption band of C-H bonds correlated with the high C content identified in the samples. These nanofibers had a lower amount of Al and Si, which agrees with the EDX results.

3.2. Dye Adsorption on PVB/Bentonite Nanofibers. The dye removal obtained for MB concentrations from 100 to 200 mg/L is shown in Figure 5. The dye adsorption capacity of this composite increased with adsorbate concentration, where the highest adsorption capacity was 63.63 mg/g at 200 mg/L. Initially, the active sites of the nanofibers were abundant and caused a fast adsorption rate of MB molecules on the composite surface [17]. The increase in the initial concentration of MB concentration provided the driving force to overcome the resistance to mass transfer between the solid and liquid phases [18]. As the active sites were occupied and the adsorbent surface was saturated, the remaining molecules underwent a repulsive interaction between the solute molecules in the solid and bulk phases [19]. These nanofibers provided active sites for the MB molecules where electrostatic interactions with the bentonite occurred. The adsorption capacity at equilibrium (q_e) ranged from 52.33 to 63.63 mg/g as the MB concentration increased from 100 to 200 mg/L. However, the adsorption efficiency dropped from 45.8% to 32.9% removal.

The visual evidence of the adsorption phenomenon for the treatment of a MB dye solution using PVB/bentonite nanofiber mat is shown in Figure 6. In particular, the polymer mat was first immersed in a MB solution with a known concentration. As time passed the formation of water films on the nanofiber mat occurred, and progressive wetting was initialized. The concentration of the dye solution started to decrease because of the adsorption process that occurred on the adsorbent. The surface of PVB/bentonite nanofibers was negatively charged and easily attracted the positively charged dye molecules. MB dye molecules saturated all available active sites of bentonite until the colour of the dye solution changed from blue to a clear solution. As for the polymer mat, the white colour coating became blue, thus confirming the maximum adsorption of dye molecules.

First, the stirring velocity was tested to determine the hydrophobic nature of the nanofibers and its impact on the overall MB removal. Figure 7 shows the adsorption results

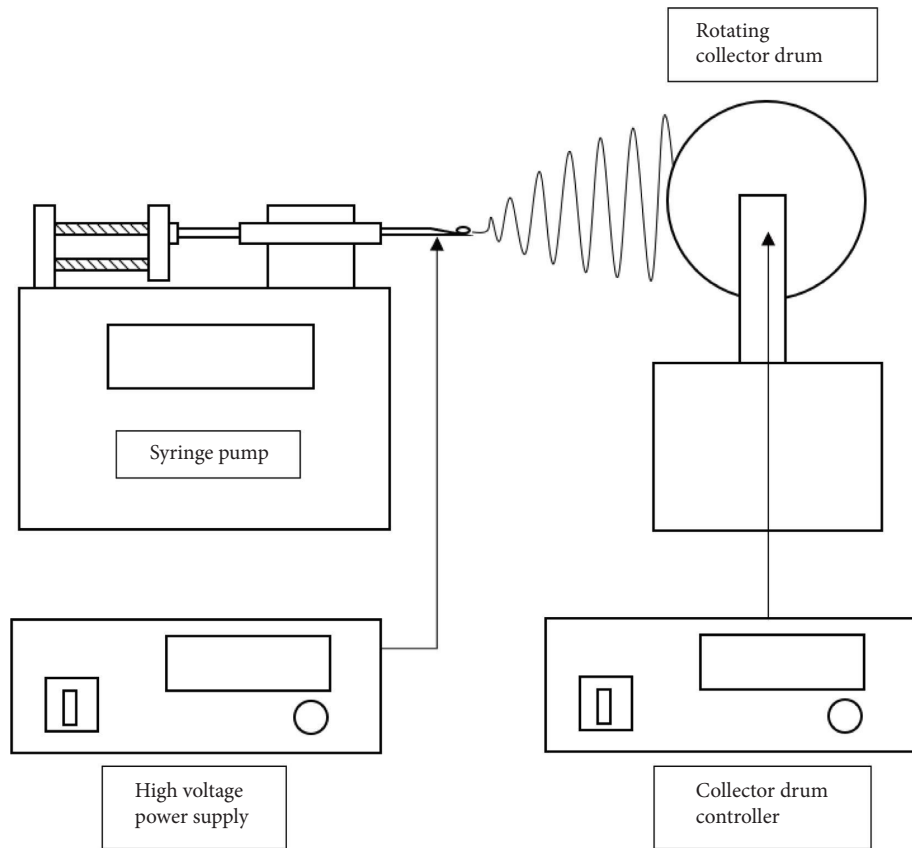


FIGURE 2: Illustration of electrospinning equipment setup to obtain PVB/bentonite nanofibers.

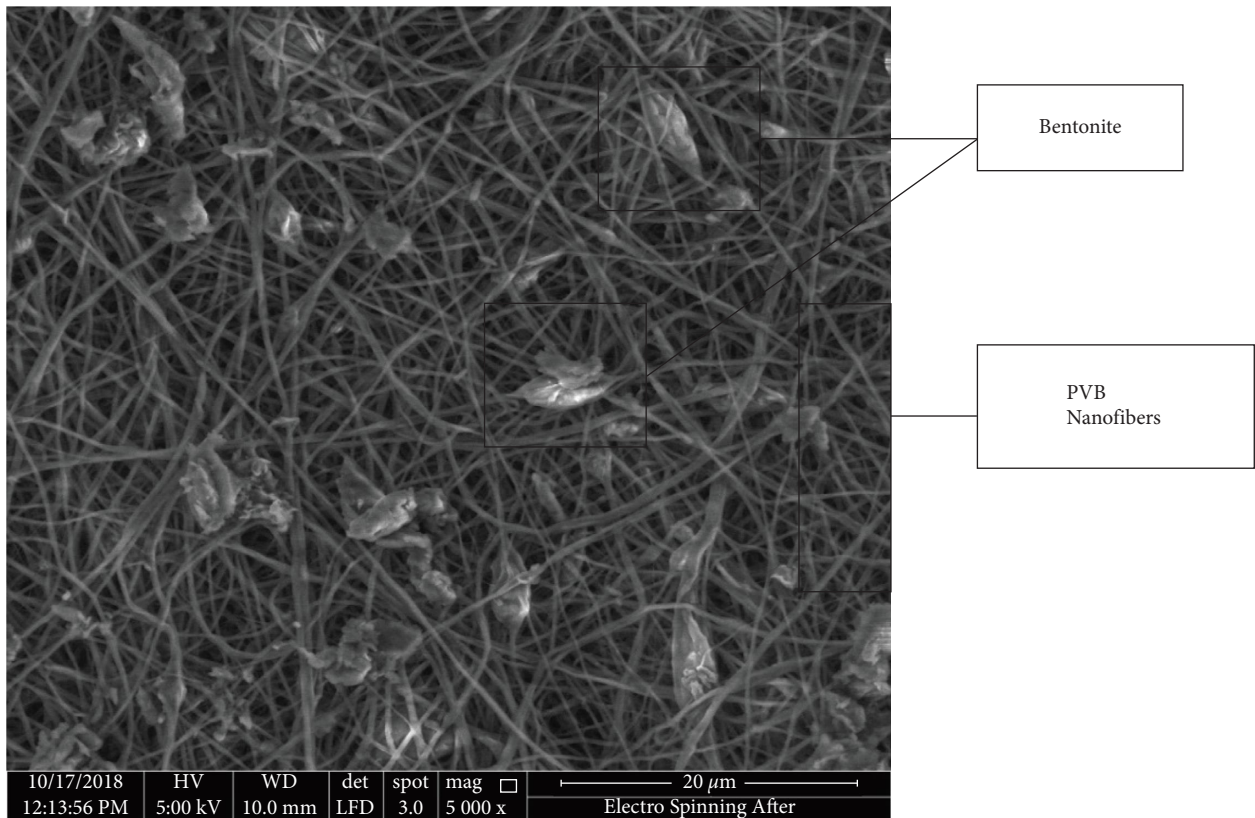


FIGURE 3: SEM/EDX of PVB/bentonite nanofibers.

TABLE 1: EDX results of PVB/bentonite nanofibers.

Element	Weight (%)	Atomic (%)
C	65.73	73.29
O	28.67	24.00
Al	1.73	0.86
Si	3.87	1.85
Total	100.0	

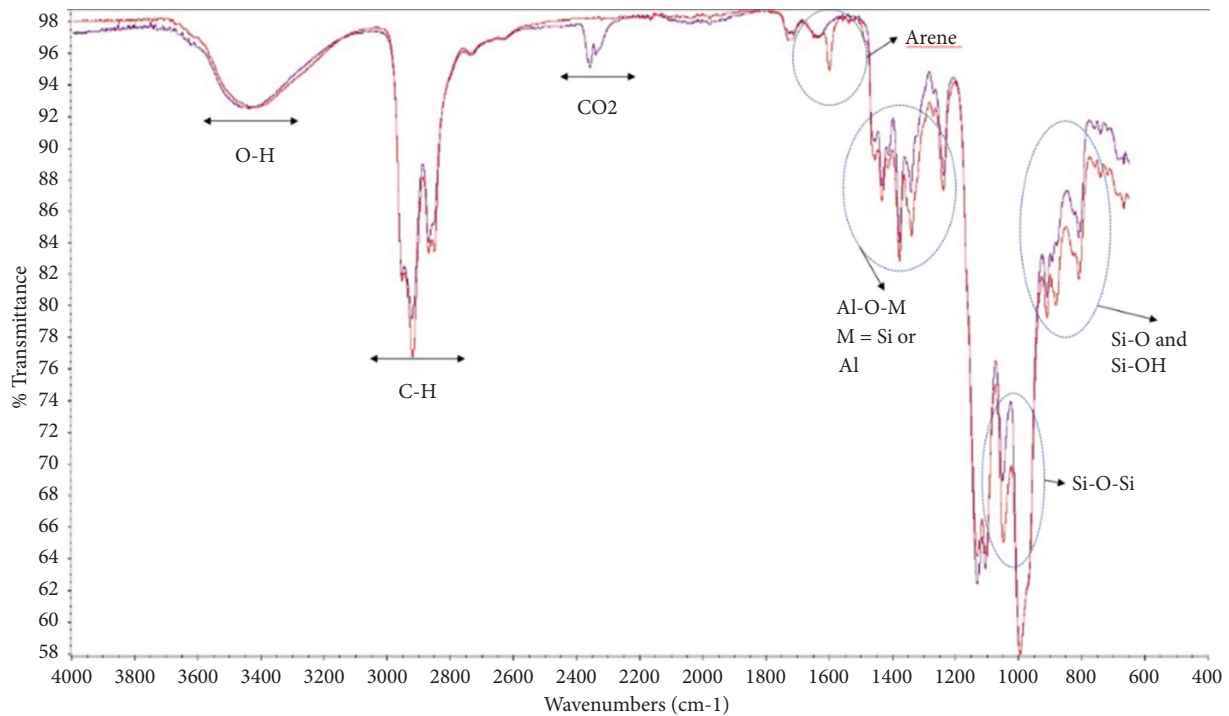


FIGURE 4: FTIR of PVB/bentonite nanofibers.

for stirring velocities of 500, 1000, and 1500 rpm using an initial dye concentration of 20 mg/L. The highest speed of 1,500 rpm generated the highest adsorption capacity of 8.31 mg/g, followed by 6.94 mg/g at 1000 rpm and 5.49 mg/g at 500 rpm. The adsorption efficiency was found to increase from 46.5% to 53.9% removal with the increase in stirring velocity.

The electrospun nanofibers are hydrophobic by nature, so they have a high resistance to water. However, these nanofibers can undergo progressive wetting. This progressive wetting is a phenomenon in which water overcomes the surface tension of nanofibers [20]. The water then passes through the pores, and the capillary forces drive the water into the narrowest pore gradually. At high stirring velocity, the amount of water exposed to the nanofibers was high, thus allowing the bentonite to encounter MB molecules and favoring their adsorption.

However, the pH of the solution could affect the adsorption capacity of these nanofibers. Adsorption studies were performed at pH levels of 3, 5, 7, 9, and 11 to analyze the impact of this operating condition, and the results are shown in Figure 8. Starting from acidic conditions, the adsorption capacity slowly increased as

the pH of the solution became more basic, from 2.58 mg/g at pH 3 to 12.25 mg/g at pH 11. The adsorption efficiency showed an increase from 53.5% to 86.6% removal. The low adsorption at low pH was due to the presence of excess H^+ ions that competed with methylene blue molecules for the active sites on the surface of nanofibers [21]. These results were consistent with those reported by Zou et al. [22], where it was found that bentonite had a low adsorption rate at low solution pH. This finding was attributed to the fact that bentonite exhibited a positively charged surface and that the MB dye molecules were repelled by their positively charged surface. At low pH, the surface of the adsorbent is closely associated with the cationic dye molecules by repulsive forces to the surface functional groups, which reduces the percentage of dye removal [23].

The effect of solution temperature on the adsorption of MB molecules from 30 to 70°C is shown in Figure 9. The dye adsorption capacity shows a decrease from 7.6 to 3.6 mg/g as the temperature increases, confirming an exothermic process. This suggests that the adsorption is physisorption in nature, and it is closely associated with the van der Waals forces and hydrogen bonding [24].

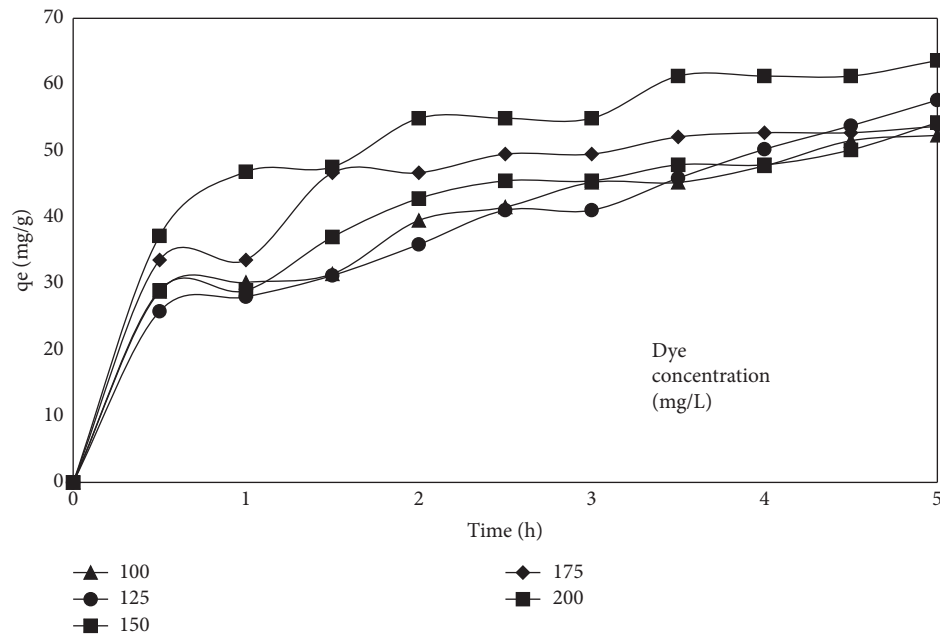


FIGURE 5: Effect of the initial concentration of the adsorbate on the MB adsorption using PVB/bentonite nanofibers at 27°C, pH 9, and 500 rpm.

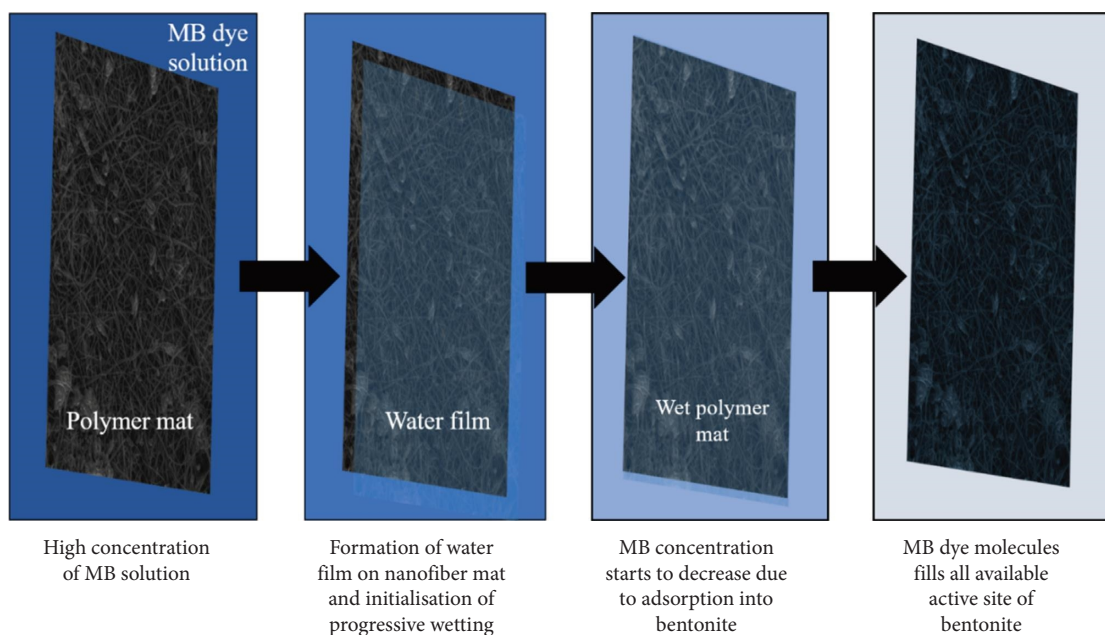


FIGURE 6: Visual evidence of the adsorption of methylene blue dye on the PVB/bentonite nanofiber mat.

Adsorption capacities of different reported adsorbents are listed in Table 2, which shows that PVB/Ben has the potential to match in effectiveness for the removal of MB from the aqueous phase.

3.3. Water Contact Angle Study. The water contact angle was measured to test the water resistance of these nanofibers. Figure 9 and Table 3 show the decrease in contact angle versus time, while Figure 10 reports the images of the water droplet undergoing progressive

wetting over time. At time = 0, the nanofibers showed a contact angle of 109.2°, indicating that they were in a hydrophobic state [28]. This hydrophobic nature affected the overall adsorption capacity of the nanofibers as prepared because it would hinder the interaction between the adsorbent surface and the adsorbate molecules. These nanofibers would prevent the MB-containing water molecules from reaching the bentonite. However, the phenomenon called progressive wetting occurred as the operating time increased. As stated, progressive wetting is a phenomenon where the polymer nanofiber loses its

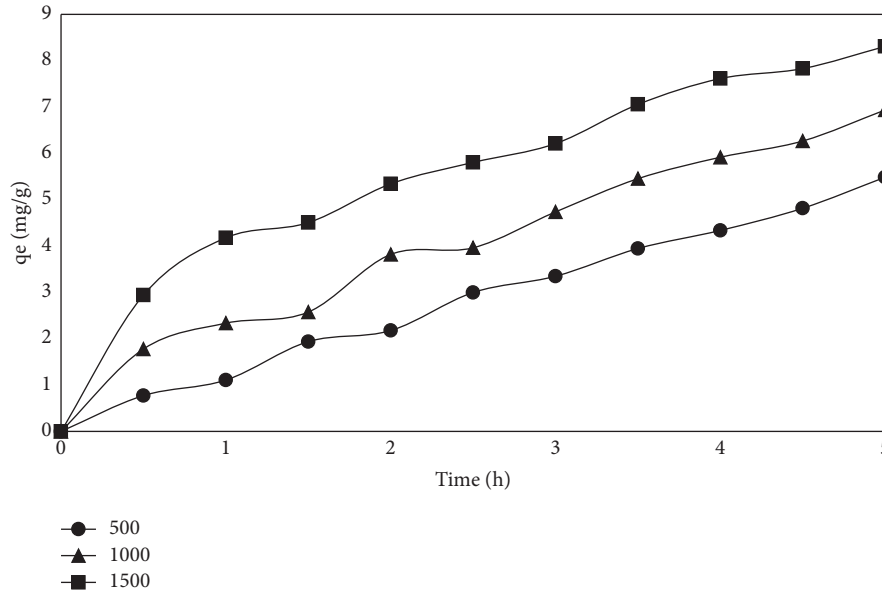


FIGURE 7: Effect of stirring velocity on the adsorption of MB molecules on PVB/bentonite nanofibers at 27°C and pH 9. Initial dye concentration of 20 mg/L.

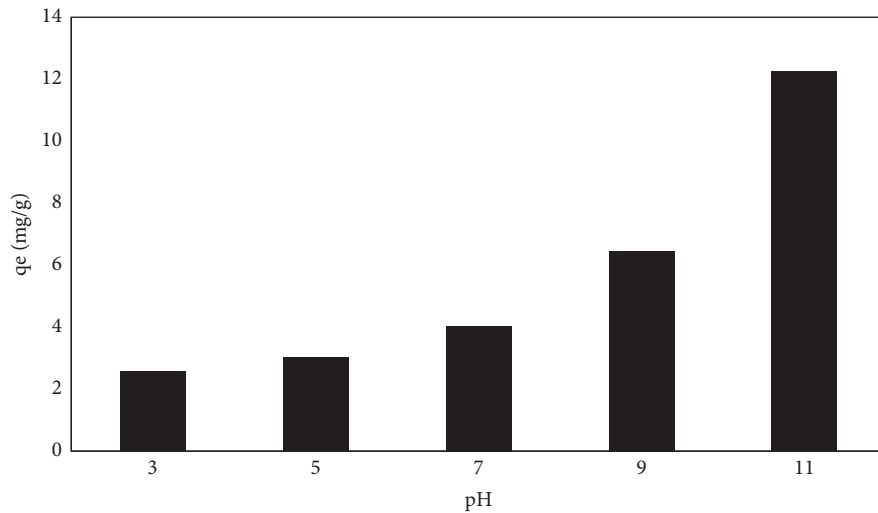


FIGURE 8: Effect of solution pH on MB molecules using PVB/bentonite nanofibers at 27°C and 500 rpm. Initial dye concentration of 20 mg/L.

hydrophobicity when the water molecules overcome the surface tension of the polymer nanofiber and the water molecules are able to go through the pore mouth and the water is driven into the narrowest pores by capillary forces [20].

A proposed phenomenon of droplets infused with MB dye passing through the nanofibers is illustrated in Figure 11. With progressive wetting, the MB dye molecules will be passed through the nanofibers and meet the bentonite. This phenomenon allowed the bentonite to adsorb the MB dye molecules from the droplets, thus finally producing a clear solution.

3.4. Thermodynamics and Kinetics Studies. MB adsorption data were analyzed by using Langmuir and Freundlich isotherm models, where the next equations were applied [29]

$$q_e = \frac{q_{\max} K_L C_e}{1 + K_L C_e},$$

$$q_e = K_F C_e^{(1/n)},$$

$$R^2 = \frac{\sum (q_{e,cal} - q_{e,ave})^2}{\sum (q_{e,cal} - q_{e,ave})^2 + \sum (q_{e,cal} - q_{e,exp})^2}, \quad (1)$$

$$ARE = \sum \left| \frac{q_{e,exp} - q_{e,cal}}{q_{e,exp}} \right|,$$

where C_e (mg/L) is the equilibrium concentration of the dye, q_e (mg/g) is the equilibrium adsorption capacity, q_{\max} (mg/g) is the theoretical maximum monolayer adsorption

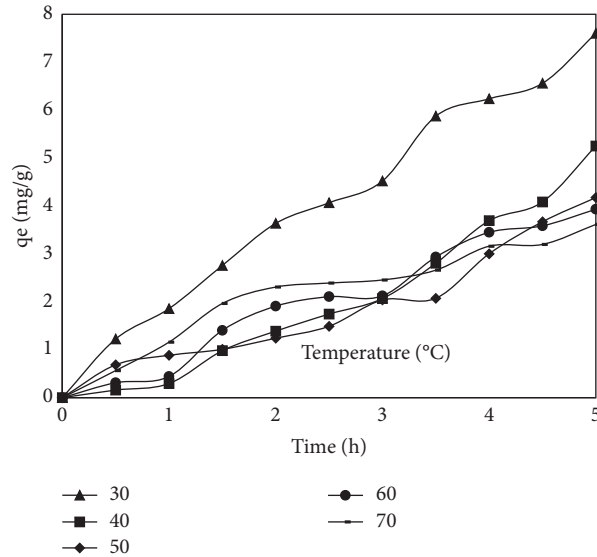


FIGURE 9: Effect of solution temperature on MB molecules using PVB/bentonite nanofibers at pH 9 and 500 rpm. Initial dye concentration of 20 mg/L.

TABLE 2: Comparison of rates of adsorption of MB in various works.

Adsorbent	Adsorption capacity (mg/g)	Reference
Peach gum polysaccharide –dodecanoyl chloride (PGP-DC)	182.61	[25]
Peach gum polysaccharide –graphene oxide (PGP-GO)	279.98	[26]
Magnetic peach gum polysaccharide (MPGP)	231.5	[27]
PVB/ben	66.63	The present study

TABLE 3: The contact angle of PVB/bentonite nanofibers versus the operating time.

Time (minute)	Contact angle
0	109.2
15	100.4
30	90.6
45	75.5
60	50.7
75	38.7
90	0

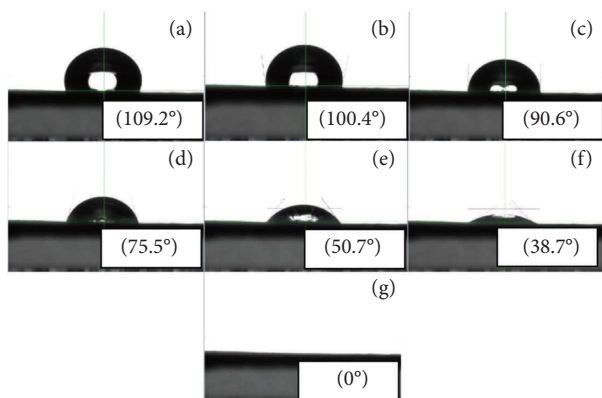


FIGURE 10: The contact angle of a water droplet on PVB/bentonite nanofibers.

capacity, K_L (L/mg) and K_F are the equilibrium constants of Langmuir and Freundlich adsorption, respectively, while n is the intensity factor. R^2 is the determination coefficient, and ARE is the average relative error. The results of the data modelling are shown in Figure 12 and Table 4. Overall, the Langmuir isotherm ($R^2 = 0.98$) suited the experimental data better than the Freundlich isotherm ($R^2 = 0.85$). The Langmuir model stated that the adsorption on the active sites of the adsorbent was homogenous in nature [30].

The adsorption rate constants of the nanofibers for different initial MB concentrations were calculated using the pseudo-first- and pseudo-second-order kinetic models. These models are defined as follows:

$$q_t = q_e(1 - e^{-K_1 t}),$$

$$q_t = \left(\frac{q_e^2 K_2 t}{1 + q_e K_2 t} \right), \quad (2)$$

where q_t and q_e are the dye adsorption capacities (mg/g) of the nanofibers at time t and equilibrium, respectively. Parameters K_1 (min^{-1}) and K_2 (g/mg-min) are the pseudo-first and pseudo-second-order kinetic constants, respectively. The calculated kinetic parameters and R^2 values are presented in Table 5. The results showed that the pseudo-second-order model ($R^2 = 0.92-0.98$) was better than the pseudo-first-order equation ($R^2 = 0.93-0.96$). The pseudo-second-order kinetic rates (K_2) ranged from 0.02 to 0.06 g/mg-min for the MB

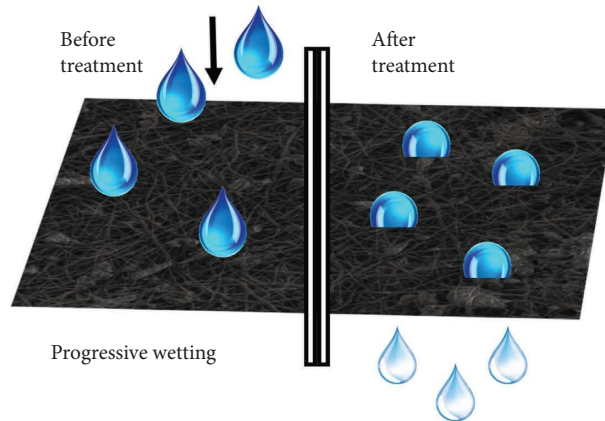


FIGURE 11: Illustration of the progressive wetting of methylene blue dye molecules onto a PVB/bentonite nanofiber mat.

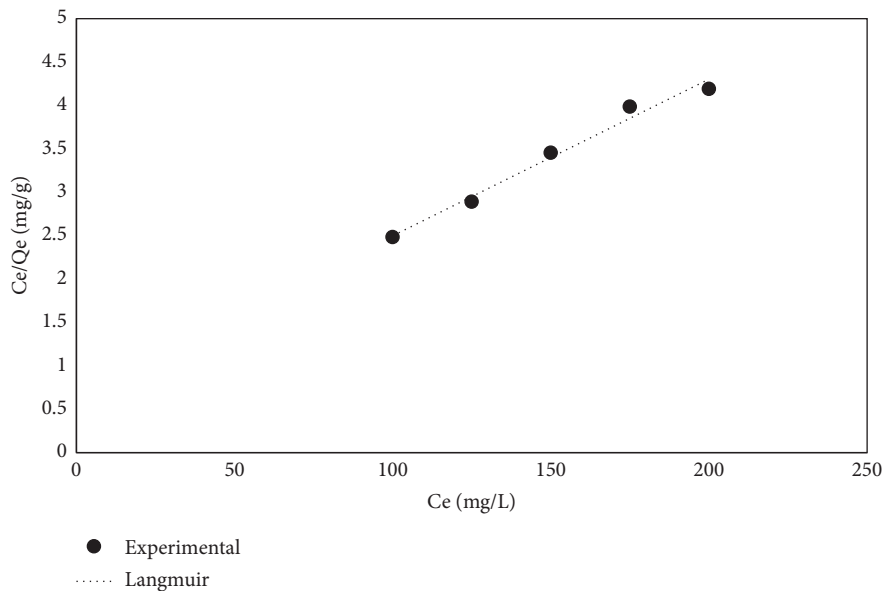


FIGURE 12: Adsorption isotherms of MB dye on PVB/bentonite nanofibers at 30°C and pH 9.

TABLE 4: Parameters of Langmuir and Freundlich isotherms for the adsorption of MB dye on the PVB/bentonite nanofibers.

Model	Parameter	Value
Langmuir	Q_m (mg/g)	55.56
	K_L (L/mg)	0.03
Freundlich	K_F (mg/g)	15.86
	N	4.92

adsorption on these nanofibers. These results indicated that chemisorption was the rate-controlling step where different adsorption sites could be involved and the adsorption rate was dependent on the concentration of the MB dye molecules on the nanofiber surface [31, 32]. The kinetic plots for the

adsorption of MB are shown in Figures 13 and 14 for pseudo-first-order and pseudo-second-order model, respectively.

The enthalpy change (H_0 , kJ/mol) for the adsorption of MB dye on these nanofibers was calculated using the following equations:

TABLE 5: Kinetic parameters for the adsorption of MB dye on PVB/bentonite nanofibers.

C_0 (mg/L)	$q_{e,exp}$ (mg/g)	Pseudo-first order model			Pseudo-second order model		
		K_1 (1/min)	$q_{e,cal}$ (mg/g)	R^2	K_2 (g/mg.min)	$q_{e,cal}$ (mg/g)	R^2
100	52.34	0.76	51.19	0.93	0.03	47.04	0.93
125	57.66	0.54	53.97	0.93	0.01	49.03	0.91
150	54.27	0.79	53.25	0.94	0.03	48.85	0.96
175	53.70	1.27	53.61	0.95	0.06	50.62	0.95
200	63.62	1.17	63.45	0.95	0.04	59.46	0.97

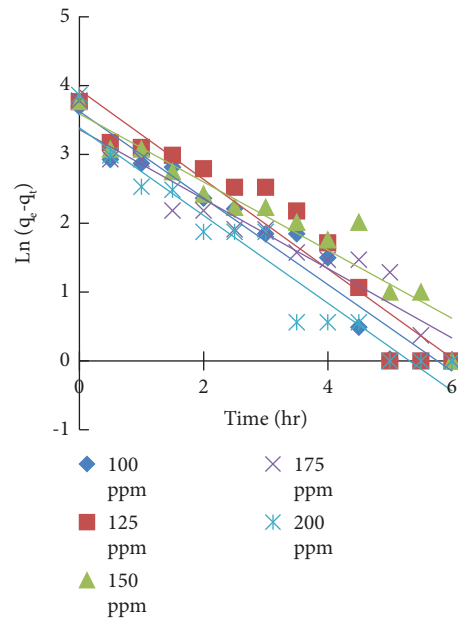


FIGURE 13: Pseudo-first-order kinetic plots for the adsorption of MB onto PVB/ben at 30°C and pH 9.

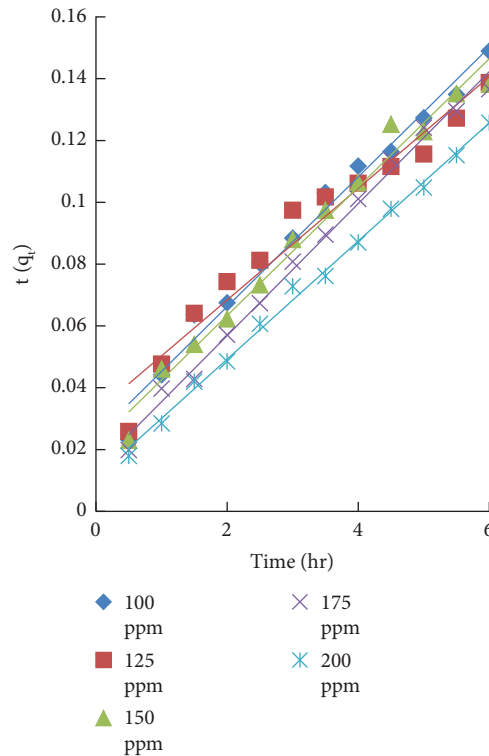


FIGURE 14: Pseudo-second-order kinetic plots for the adsorption of MB onto PVB/ben at 30°C and pH 9.

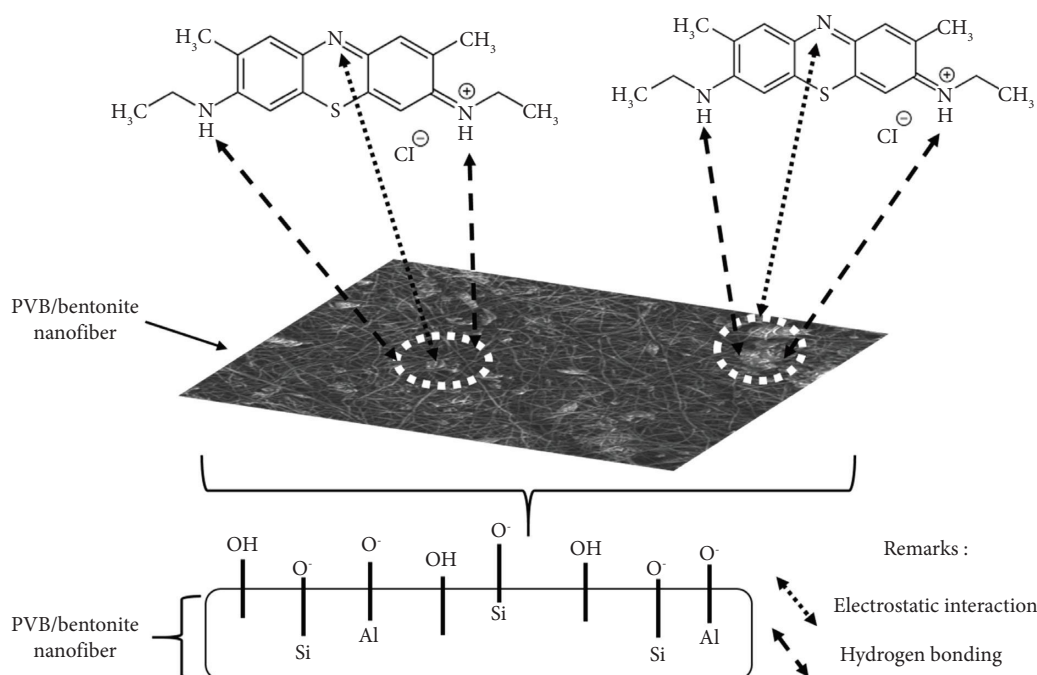


FIGURE 15: Adsorption mechanism of methylene blue dye on PVB/bentonite nanofibers.

$$K_d = \frac{(C_0 - C_e) \cdot V}{mC_e},$$

$$\Delta G_0 = -RT \ln K_d, \quad (3)$$

$$\ln K_d = \frac{\Delta S^0}{R} + \frac{\Delta H^0}{RT},$$

where ΔH^0 was obtained from the results of equilibrium experiments performed at 303, 313, 323, and 333 K. Calculated adsorption enthalpy was -27.724 kJ/mol, thus indicating an exothermic dye adsorption process, which could involve electrostatic interactions and hydrogen bonding [31].

3.5. Dye Adsorption Mechanism. The mechanism of adsorption of MB dye on PVB/bentonite nanofiber mat can be ascribed to the electrostatic attraction between positively charged dye molecules and the negatively charged groups of Si-O⁻ and Al-O⁻ that were present on the surface of the polymer mat (Figure 15). The charged groups of silica and alumina were the main constituents of the dispersed bentonite particles in the adsorbent formulation. These elements could play an important role in the adsorption of the MB dye. The hydrophobic and hydrogen bonding interactions might be the other possible interactions involved in the adsorption of this organic pollutant. The hydroxyl groups (-OH) might form hydrogen bonds with the -NH₂ groups of dye molecules.

4. Conclusions

Bentonite was successfully utilized to prepare a polymer-based composite using PVB and electrospun. This PVB/

bentonite composite was obtained in the form of nanofibers and tested for the adsorption of MB dye from an aqueous solution. SEM/EDX analysis showed that bentonite was successfully attached to the nanofiber in a low concentration. The adsorption properties of these composite nanofibers were affected by the process operating conditions (i.e., stirring velocity, pH, temperature, and adsorbate concentration), where pH and temperature played the most significant role in dye removal. Methylene blue adsorption on these nanofibers was exothermic, where van der Waals forces, hydrogen bonding, and electrostatic interactions could play a major role in the adsorption mechanism. The pseudo-second-order kinetic and Langmuir isotherm were the best models to fit the MB dye adsorption experimental data. The highest dye adsorption was 66.63 mg/g at pH 9 and 303 K. This novel composite is an interesting and promising material for developing low-cost and effective adsorption processes for the treatment of wastewater caused by dye molecules.

Data Availability

The data used to support the findings of this study are available from the corresponding author upon request.

Ethical Approval

The manuscript does not involve research about humans and animals.

Conflicts of Interest

The authors declare that they have no conflicts of interest.

Authors' Contributions

All authors contributed to the conception and design. Material preparation, data collection, and analysis were performed by Aiizat Ikhwan Abdul Jalil. The first draft of the manuscript was written by Aiizat Ikhwan Abdul Jalil, and all other authors, Syahida Farhan Azha, Adrian Bonilla Petriciolet, Mohammad Shahadat, and Suzylawati Ismail, commented on previous versions of the manuscript. All authors read and approved the final manuscript. All authors participated in the drafting of this manuscript. All authors agreed to publish this manuscript.

Acknowledgments

The authors would like to acknowledge the Ministry of Higher Education of Malaysia for the Fundamental Research Grant Scheme with project code FRGS/1/2018/TK02/USM/02/6 for funding this research project. The authors also acknowledge Universiti Sains Malaysia for support throughout this research work.

References

- [1] R. R. Pawar, H. C. Bajaj, H. C. Bajaj, and S. M. Lee, "Activated bentonite as a low-cost adsorbent for the removal of Cu(II) and Pb(II) from aqueous solutions: batch and column studies," *Journal of Industrial and Engineering Chemistry*, vol. 34, pp. 213–223, 2016.
- [2] Ö Şahin, M. Kaya, and C. Saka, "Plasma-surface modification on bentonite clay to improve the performance of adsorption of methylene blue," *Applied Clay Science*, vol. 116–117, pp. 46–53, 2015.
- [3] S. F. Azha, M. Shahadat, and S. Ismail, "Acrylic polymer emulsion supported bentonite clay coating for the analysis of industrial dye," *Dyes and Pigments*, vol. 145, pp. 550–560, 2017.
- [4] S. Hong, C. Wen, J. He, F. Gan, and Y. S. Ho, "Adsorption thermodynamics of methylene blue onto bentonite," *Journal of Hazardous Materials*, vol. 167, no. 1–3, pp. 630–633, 2009.
- [5] Z. H. Diao, X. R. Xu, H. Chen et al., "Simultaneous removal of Cr(VI) and phenol by persulfate activated with bentonite-supported nanoscale zerovalent iron: reactivity and mechanism," *Journal of Hazardous Materials*, vol. 316, pp. 186–193, 2016.
- [6] X. You, J. Cao, X. Liu, J. Lu, and X. Chen, "Synthesis of the poly(acrylic acid-acrylic sodium) bentonite composite and its adsorption of Cd(II)," *Asia-Pacific Journal of Chemical Engineering*, vol. 12, no. 1, pp. 65–74, 2017.
- [7] P. Peer, M. Stenicka, V. Pavlinek, P. Filip, I. Kuritka, and J. Brus, "An electrorheological investigation of PVB solutions in connection with their electrospinning qualities," *Polymer Testing*, vol. 39, pp. 115–121, 2014.
- [8] E. Ceretti, P. S. Ginestra, M. Ghazinejad, A. Fiorentino, and M. Madou, "Electrospinning and characterization of polymer-graphene powder scaffolds," *CIRP Annals*, vol. 66, no. 1, pp. 233–236, 2017.
- [9] M. Stenicka, P. Peer, P. Filip, V. Pavlinek, and M. Machovsky, "Electrospinning of PVB solved in methanol and isopropanol," in *Proceedings of the 5th WSEAS International Conference on Materials Science*, pp. 239–243, 2012.
- [10] L. J. Chen, J. D. Liao, S. J. Lin, Y. J. Chuang, and Y. S. Fu, "Synthesis and characterization of PVB/silica nanofibers by electrospinning process," *Polymer*, vol. 50, no. 15, pp. 3516–3521, 2009.
- [11] F. Yener and B. Yalcinkaya, "Electrospinning of polyvinyl butyral in different solvents," *E-Polymers*, vol. 13, pp. 1–14, 2013.
- [12] A. I. A. Jalil and S. Ismail, "Adsorption of methylene blue via electrospun polyvinyl butyral/bentonite," in *Proceedings of the 6th International Conference on Environment (ICENV2018)*, New York, NY, USA, July 2019.
- [13] B. J. Mullins, I. E. Agranovski, R. D. Braddock, and C. M. Ho, "Effect of fiber orientation on fiber wetting processes," *Journal of Colloid and Interface Science*, vol. 269, no. 2, pp. 449–458, 2004.
- [14] Y. Yin and J. Xiong, "Effect of the distribution of fiber orientation on the mechanical properties of silk fibroin/polycaprolactone nanofiber mats," *Journal of Engineered Fibers and Fabrics*, vol. 12, no. 3, Article ID 155892501701200303, 2017.
- [15] M. Wawrzekiewicz, M. Wiśniewska, V. M. Gun'ko, and V. I. Zarko, "Adsorptive removal of acid, reactive and direct dyes from aqueous solutions and wastewater using mixed silica-alumina oxide," *Powder Technology*, vol. 278, pp. 306–315, 2015.
- [16] M. Wawrzekiewicz, M. Wiśniewska, A. Wołowicz, V. M. Gun'ko, and V. I. Zarko, "Mixed silica-alumina oxide as sorbent for dyes and metal ions removal from aqueous solutions and wastewaters," *Microporous and Mesoporous Materials*, vol. 250, pp. 128–147, 2017.
- [17] M. Auta and B. H. Hameed, "Chitosan-clay composite as highly effective and low-cost adsorbent for batch and fixed-bed adsorption of methylene blue," *Chemical Engineering Journal*, vol. 237, pp. 352–361, 2014.
- [18] B. M. Thamer, H. El-Hamshary, S. S. Al-Deyab, and M. H. El-Newehy, "Functionalized electrospun carbon nanofibers for removal of cationic dye," *Arabian Journal of Chemistry*, vol. 12, no. 6, pp. 747–759, 2019.
- [19] M. I. Khan, S. Zafar, M. F. Azhar et al., "Leaves powder of syzgium cumini as an adsorbent for removal of Congo red dye from aqueous solution," *Fresenius Environmental Bulletin*, Sliema, Malta, vol. 27, pp. 3342–3350, 2018.
- [20] E. Guillen-Burrieza, M. O. Mavukkandy, M. R. Bilad, and H. A. Arafat, "Understanding wetting phenomena in membrane distillation and how operational parameters can affect it," *Journal of Membrane Science*, vol. 515, pp. 163–174, 2016.
- [21] J. Chang, J. Ma, Q. Ma et al., "Adsorption of methylene blue onto Fe₃O₄/activated montmorillonite nanocomposite," *Applied Clay Science*, vol. 119, pp. 132–140, 2016.
- [22] C. Zou, W. Jiang, J. Liang, X. Sun, and Y. Guan, "Removal of Pb(II) from aqueous solutions by adsorption on magnetic bentonite," *Environmental Science & Pollution Research*, vol. 26, no. 2, pp. 1315–1322, 2019.
- [23] A. T. Adeolu, O. T. Okareh, and A. O. Dada, "Adsorption of chromium ion from industrial effluent using activated carbon derived from plantain (musa paradisiaca) wastes," *American Journal of Environmental Protection*, vol. 4, pp. 7–20, 2016.
- [24] L. Sellaoui, F. Dhaouadi, Z. Li et al., "Implementation of a multilayer statistical physics model to interpret the adsorption of food dyes on a chitosan film," *Journal of Environmental Chemical Engineering*, vol. 9, no. 4, Article ID 105516, 2021.
- [25] S. Zeng, J. Tan, X. Xu, X. Huang, and L. Zhou, "Facile synthesis of amphiphilic peach gum polysaccharide as a robust host for efficient encapsulation of methylene blue and methyl

- orange dyes from water,” *International Journal of Biological Macromolecules*, vol. 154, pp. 974–980, 2020.
- [26] S. Zeng, J. Long, J. Sun, G. Wang, and L. Zhou, “A review on peach gum polysaccharide: hydrolysis, structure, properties and applications,” *Carbohydrate Polymers*, vol. 279, Article ID 119015, 2022.
- [27] C. Li, X. Wang, D. Meng, and L. Zhou, “Facile synthesis of low-cost magnetic biosorbent from peach gum polysaccharide for selective and efficient removal of cationic dyes,” *International Journal of Biological Macromolecules*, vol. 107, pp. 1871–1878, 2018.
- [28] N. Nuraje, W. S. Khan, Y. Lei, M. Ceylan, and R. Asmatulu, “Superhydrophobic electrospun nanofibers,” *Journal of Materials Chemistry*, vol. 1, no. 6, pp. 1929–1946, 2013.
- [29] M. S. Shamsudin, S. F. Azha, L. Sellaoui et al., “Fabrication and characterization of a thin coated adsorbent for antibiotic and analgesic adsorption: experimental investigation and statistical physical modelling,” *Chemical Engineering Journal*, vol. 401, Article ID 126007, 2020.
- [30] K. Chinoune, K. Bentaleb, Z. Boubberka, A. Nadim, and U. Maschke, “Adsorption of reactive dyes from aqueous solution by dirty bentonite,” *Applied Clay Science*, vol. 123, pp. 64–75, 2016.
- [31] F. Liu, X. Wang, B. Y. Chen, S. Zhou, and C. T. Chang, “Removal of Cr(VI) using polyacrylonitrile/ferrous chloride composite nanofibers,” *Journal of the Taiwan Institute of Chemical Engineers*, vol. 70, pp. 401–410, 2017.
- [32] R. Sahraei, Z. Sekhavat Pour, and M. Ghaemy, “Novel magnetic biosorbent hydrogel beads based on modified gum tragacanth/graphene oxide: removal of heavy metals and dyes from water,” *Journal of Cleaner Production*, vol. 142, pp. 2973–2984, 2017.